Available online at www.sciencedirect.com
ScienceDirect
Journal of Photochemistry and Photobiology A: Chemistry 187 (2007) 269–274
Journal of Photochemistry and Photobiology A:Chemistry
www.elsevier.com/locate/jphotochem

Photoreversible cyclisation of a 3-(2-benzylbenzoyl)-quinolinone: A highly efficient photochromic compound

J. Berthet [a], J.-C. Micheau [b], V. Lokshin [c], M. Vales [c], A. Samat [c], G. Vermeersch [a], S. Delbaere [a,*]

[a] *CNRS UMR 8009, Université de Lille 2, Faculté de Pharmacie, F-59006 Lille Cedex, France*
[b] *CNRS UMR 5623, Université Paul Sabatier, IMRCP, F-31062 Toulouse, France*
[c] *CNRS UMR 6114, Université de la Méditerranée, Faculté des Sciences de Luminy, 13288 Marseille Cedex 9, France*

Received 13 September 2006; received in revised form 29 September 2006; accepted 9 October 2006
Available online 10 November 2006

Abstract

NMR and kinetic study of the photochromism of the 3-(2-benzylbenzoyl)-2-ethyl-1-methyl-4(1H)-quinolinone (**P_0**) is reported. Under UV irradiation, two thermally stable but photochemically reversible diastereomeric benzoacridinones (**P_1** and **P_2**) are formed. Kinetic analysis shows that under UV, all the six possible reversible paths between **P_0**, **P_1** and **P_2** are operative, while under visible irradiation, only thermally irreversible photoketonizations from **P_1** and **P_2** toward **P_0** occur. Temperature effects on the **P_1**/**P_2** ratio and on the rates of photoketonization are evidenced. The presence of thermal activation barriers is assumed to interpret these observations.

Keywords: Photochromism; Quinolinone; NMR spectroscopy

1. Introduction

Aryl ketones with *o*-alkyl groups are known to undergo a highly efficient photoinduced enolisation [1–3]. The triplet states of ketones are transformed into triplet biradicals via hydrogen abstraction. Biradicals decay to Z- and E-isomers of the corresponding dienol in the ground state [4,5]. Dienols can thermally return-back to the starting ketones or stereoselectively cyclise [4,6,7], unless trapped with dienophiles or acid [1]. The distribution of products from biradicals has therefore drawn much attention in terms of conformational preferences that pre-exist in the biradicals [8–11]. Outside this purely theoretical aspect, photoenolisation can find applications in photochromism, but to the best of our knowledge, with the exception of some reports [12,13], no attention has been paid toward exploring carbonyl compounds in solution as photochromic materials. Recently, we reported the structural and kinetic investigation of the photochromic 3-benzoyl-2-benzyl-6,7-difluoro-1-propyl-1H-quinolin-4-one (**1**). Under UV irradiation, two thermally reversible photoenols were produced, but photodegradation also occurred [14]. On the contrary, irradiation of a parent molecule, 3-(2-benzylbenzoyl)-1,2-dimethyl-4(1H)-quinolinone (**2**), leads to the photoreversible formation of hydroxy substituted dihydrobenzoacridinone, which can thermally and reversibly rearrange into his diketo isomers [15]. As the substituents have a strong effect on the course of reaction, we replaced one of the methyl by an ethyl group in **2**. The reactivity under UV then under visible irradiation of the 3-(2-benzylbenzoyl)-2-ethyl-1-methyl-4(1H)-quinolinone (**P_0**) was therefore deeply investigated by NMR spectroscopy (Scheme 1).

2. Experimental

2.1. Materials

The compound **P_0** (colourless crystals, m.p. 166 °C) had previously been synthesised by some of us [16].

2.2. NMR investigations and experimental conditions

Thermostated samples (concentration = 1×10^{-3} M in degassed toluene-d_8) were irradiated directly in the NMR tube

* Corresponding author. Tel.: +33 3 20 96 40 13; fax: +33 3 20 95 90 09.
E-mail address: stephanie.delbaere@univ-lille2.fr (S. Delbaere).

1010-6030/$ – see front matter © 2006 Elsevier B.V. All rights reserved.
doi:10.1016/j.jphotochem.2006.10.009

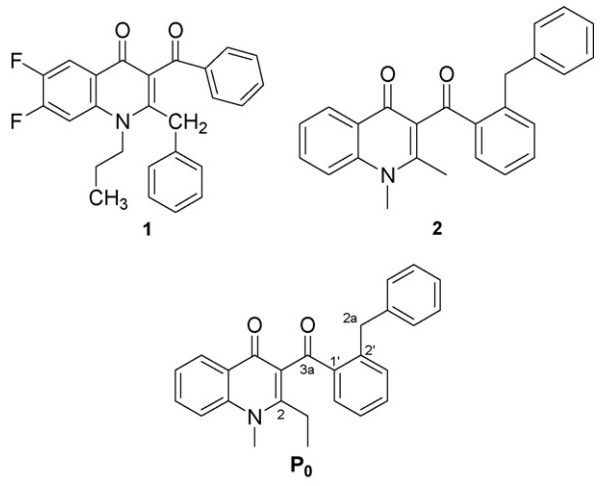

Scheme 1.

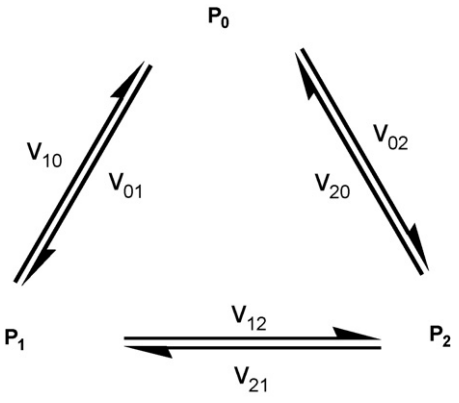

Scheme 2.

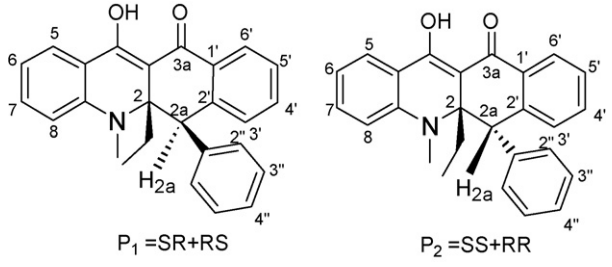

Scheme 3. Structure and numbering of $\mathbf{P_1}$ and $\mathbf{P_2}$.

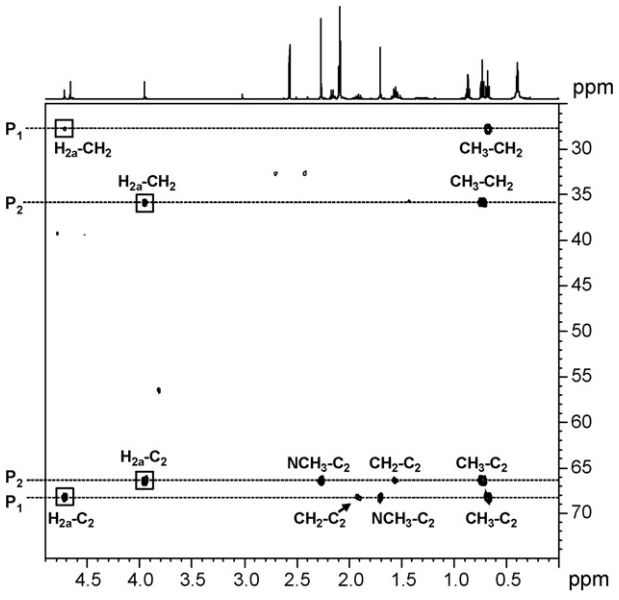

Fig. 2. Part of ^{1}H–^{13}C-NMR HMBC with connections characterizing cyclization.

(5 mm), using a 1000 W Xe–Hg HP filtered (Schott 011FG09, $259 < \lambda < 388$ nm with $\lambda_{max} = 330$ nm, $T = 79\%$ and oriel 3–74, $\lambda > 400$ nm $T = 87\%$) short-arc lamp (oriel). After each irradiation period (60 s), the sample was rapidly transferred into the thermoregulated probe of a Bruker Avance-DPX NMR spectrometer (^{1}H, 300 MHz).

Degassing of solution to remove oxygen was made by the technique of freeze-pump-thaw cycles (five cycles, 2.25×10^{-6} Torr) directly in the Young valve NMR sample tubes (Wilmad 507-JY-7).

2.3. Data analysis

The calculated evolution in concentrations was obtained by numerical integration of the set of differential equations written from a three-species system (Scheme 2), using homemade curve fitting software [17].

The rate equations have been assumed to be first-order-like with $v_{ij} = h_{ij}[X_i]$, where $h_{ij} = \Phi_{ij}\varepsilon_i I_0 F$.

Φ_{ij} is the quantum yield of the global photochemical reaction of compound "X_i" into compound "X_j", ε_i is the molar absorp-

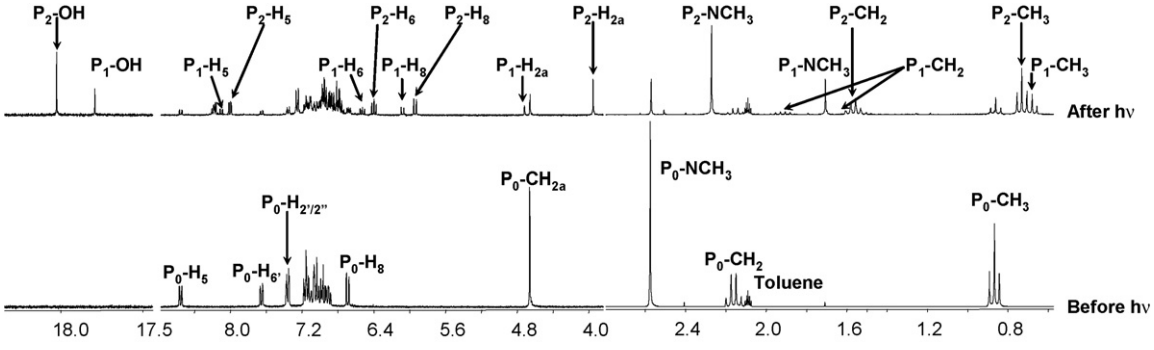

Fig. 1. ^{1}H-NMR spectra of $\mathbf{P_0}$ before and after UV irradiation at 295 K.

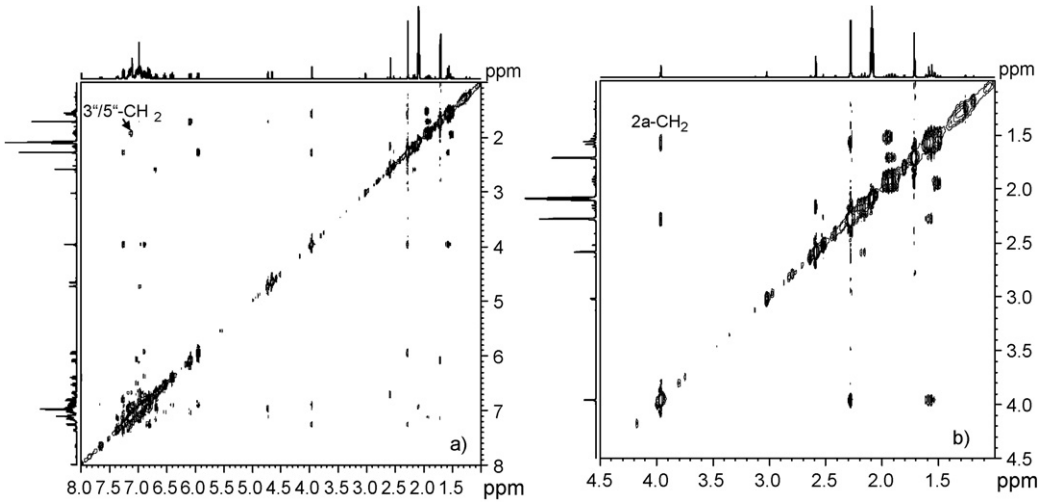

Fig. 3. Part of ^{1}H–^{1}H-NMR Roesy with characteristic dipolar contacts in (a) $\mathbf{P_1}$, (b) $\mathbf{P_2}$.

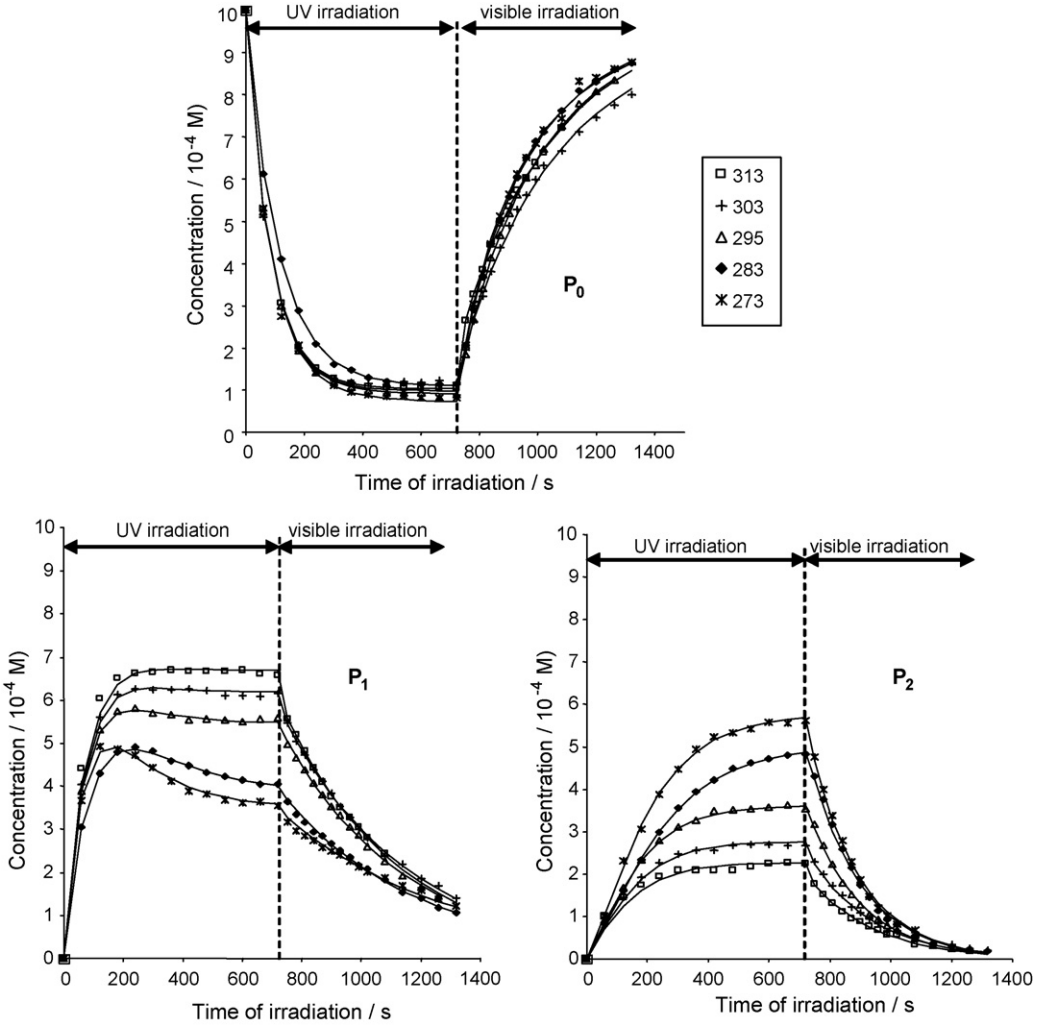

Fig. 4. Photocolouration under UV irradiation and photobleaching under visible irradiation kinetics at five temperatures (signs are experimental concentrations; solid lines are fitted curves using our mechanistic model).

Table 1
Results from kinetic analysis of photocolouration and photobleaching processes

	$T = 273$ K	$T = 283$ K	$T = 295$ K	$T = 303$ K	$T = 313$ K
$^{UV}h_{01}$	10.1×10^{-3}	7.1×10^{-3}	10.2×10^{-3}	10.6×10^{-3}	11.7×10^{-3}
$^{UV}h_{10}$	1.4×10^{-3}	1.9×10^{-3}	1.7×10^{-3}	2.2×10^{-3}	2.4×10^{-3}
$^{UV}h_{02}$	1.3×10^{-3}	1.2×10^{-3}	1.2×10^{-3}	1.5×10^{-3}	2.4×10^{-3}
$^{UV}h_{20}$	7.1×10^{-4}	4.4×10^{-4}	1.7×10^{-4}	1.3×10^{-4}	1.0×10^{-4}
$^{UV}h_{12}$	4.3×10^{-3}	2.6×10^{-3}	3.3×10^{-3}	2.4×10^{-3}	1.1×10^{-3}
$^{UV}h_{21}$	2.1×10^{-3}	1.6×10^{-3}	5.2×10^{-3}	6.0×10^{-3}	4.4×10^{-3}
$[\mathbf{P_0}]_e$	8.1×10^{-5}	1.3×10^{-4}	8.8×10^{-5}	1.2×10^{-4}	1.2×10^{-4}
$[\mathbf{P_1}]_e$	3.6×10^{-4}	3.8×10^{-4}	5.6×10^{-4}	6.2×10^{-4}	6.6×10^{-4}
$[\mathbf{P_2}]_e$	5.6×10^{-4}	4.9×10^{-4}	3.5×10^{-4}	2.7×10^{-4}	2.3×10^{-4}
$[\mathbf{P_1}]_e/[\mathbf{P_2}]_e$	0.64	0.78	1.6	2.3	2.9
$^{Vis}h_{10}$	1.9×10^{-3}	2.2×10^{-3}	2.4×10^{-3}	2.4×10^{-3}	2.6×10^{-3}
$^{Vis}h_{20}$	6.1×10^{-3}	5.9×10^{-3}	5.7×10^{-3}	4.8×10^{-3}	4.7×10^{-3}

$^{UV}h_{ij}$: apparent first order rate constant (s^{-1}) of the process $i \rightarrow j$ under UV irradiation, $[X_i]_e$: concentration in mol L^{-1} at the end of UV irradiation, $^{Vis}h_{ij}$: apparent first order rate constant (s^{-1}) of the process $i \rightarrow j$ under visible light irradiation.

tion coefficient of compound X_i at the irradiation wavelength, l the optical path, I_0 the incident photon flux and F is the photokinetic factor, which has been assumed to remain constant in these experiments. This assumption is fully justified if F is strictly constant. As the irradiation light was not strictly monochromatic, Φ_{ij} and ε_i values must be considered as wavelength-averaged. Then, h_{ij} terms correspond to apparent first order rate constants.

According to Scheme 2, the following set of differential equations has been used:

$$\frac{d[\mathbf{P_0}]}{dt} = v_{10} + v_{20} - v_{01} - v_{02},$$

$$\frac{d[\mathbf{P_1}]}{dt} = v_{01} + v_{21} - v_{10} - v_{12}$$

together with the mass balance equation: $[\mathbf{P_0}] + [\mathbf{P_1}] + [\mathbf{P_2}] = [\mathbf{P_0}]_0$ where $[\mathbf{P_0}]_0$ is the initial concentration of the quinolinone. Each temperature was analysed independently.

3. Results

3.1. Structural identification of photoproducts

UV irradiation of a degassed toluene-d_8 solution of $\mathbf{P_0}$ at 295 K led only to two photoproducts, $\mathbf{P_1}$ and $\mathbf{P_2}$ which were thermally stable but photoreversible under visible light. By 1 and 2D NMR experiments, they were identified as two cyclised diastereomeric acridinone derivatives (Scheme 3). In the ^{1}H-NMR spectrum (Fig. 1), the singlet signals at 4.72 and 17.85 ppm, and at 3.99 and 18.1 ppm are assigned to proton H_{2a} and OH function, in $\mathbf{P_1}$ and $\mathbf{P_2}$, respectively. The downfield shift of OH is explained by hydrogen bonding with the carbonyl group. HMBC correlations H_{2a}–C_{CH_2} and H_{2a}–C_2 prove that both carbons C_2 and C_{2a} in $\mathbf{P_1}$ and $\mathbf{P_2}$ are directly connected (Fig. 2). By ^{1}H–^{1}H Roesy experiment (Fig. 3), the exact configuration of diastereomeric carbons 2 and 2a was attributed to be (SR + RS) for $\mathbf{P_1}$ and (SS + RR) for $\mathbf{P_2}$ [18]. No thermal conversion toward acridine-dione derivatives or other detectable compounds was observed.

3.2. Photocolouration and photobleaching kinetics

The course of the photoreaction under UV then visible irradiation was investigated at five temperatures (273, 283, 295, 303 and 313 K). After each irradiation period, ^{1}H-NMR spectra were recorded, and then another irradiation period was resumed. When the photostationary state had been reached, the sample was irradiated in the same way with visible light. By measuring several specific NMR peak-intensities, the time-evolution of the concentrations of $\mathbf{P_0}$, $\mathbf{P_1}$ and $\mathbf{P_2}$ can be plotted (Fig. 4).

The most simple and general mechanism to describe the macroscopic evolution of the three products is given in the Scheme 2, where $\mathbf{P_0}$, $\mathbf{P_1}$ and $\mathbf{P_2}$ are connected by six photoreversible paths.

Under UV irradiation, it is necessary to consider the six processes in order to obtain satisfactory fit between experimental data and calculated curves. On the other hand, under visible light, the simplest way to fit our kinetics is to assume that $\mathbf{P_1}$ and $\mathbf{P_2}$ return directly to the initial quinolinone $\mathbf{P_0}$ by parallel paths. This assumption is justified because in these conditions, $\mathbf{P_0}$ does not absorb. The extracted apparent rate constants $^{UV}h_{ij}$ and $^{Vis}h_{ij}$ are gathered in Table 1.

4. Discussion and conclusion

From the structural observations, UV irradiation results in cyclisation to six-member rings. As no cyclobutanols derivatives were observed, we can reasonably suggest that UV irradiation leads via hydrogen abstraction to the formation of a 1,6-biradical [19]. It is likely that biradical $Bi_{1–6(O)}$ does not cyclise as photoproducts resulting from bond-formation between carbons C_2 and C_{2a} are formed. This implies a rearrangement of biradical $Bi_{1–6(O)}$ into $B_{1–6(N)}$, followed by a rotation around the bond $C_{1'}$–C_{3a} towards $B_{1–6(N1)}$ and $B_{1–6(N2)}$, the precursors of $\mathbf{P_1}$ and $\mathbf{P_2}$, respectively (Scheme 4).

Most of the apparent first order rate constants h_{ij} that have been extracted from the numerical kinetic modelling of the concentration versus time curves under UV irradiation do not show any clear-cut temperature effect. However, a more careful examination shows some significant trends. When the temper-

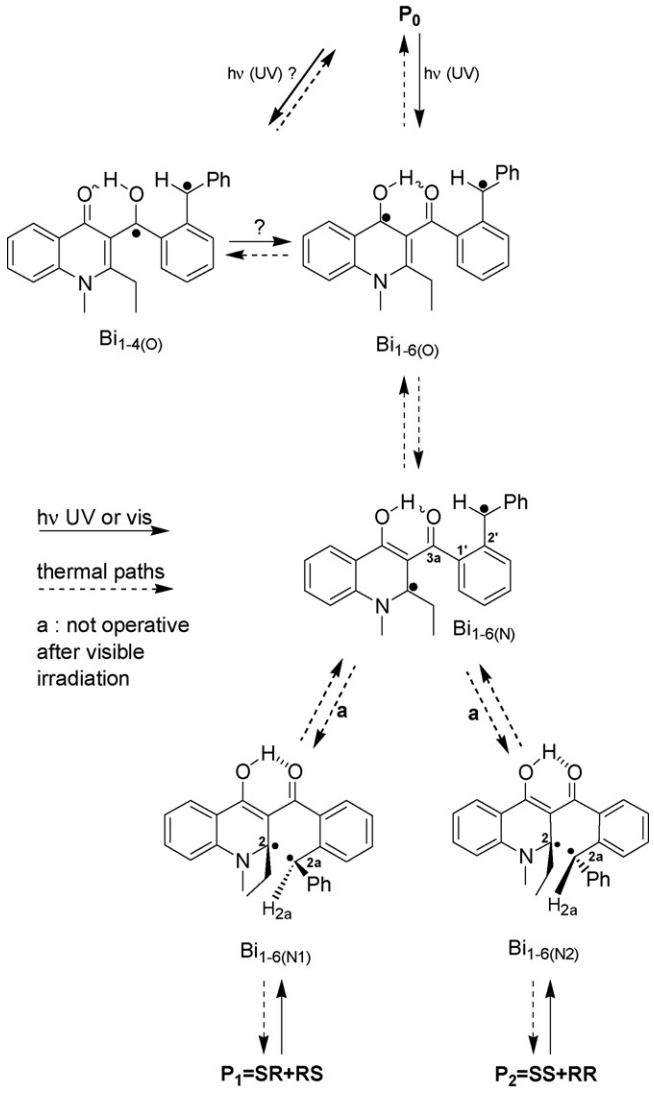

Scheme 4.

ature increases, ${}^{UV}h_{10}$ slightly but significantly increases while ${}^{UV}h_{20}$ decreases. Moreover, it appears that $\mathbf{P_0}$ goes preferentially towards $\mathbf{P_1}$, as the corresponding rate ${}^{UV}h_{01}$ ($\mathbf{P_0} \rightarrow \mathbf{P_1}$) is always higher than ${}^{UV}h_{02}$ ($\mathbf{P_0} \rightarrow \mathbf{P_2}$). Consequently, the biradical $Bi_{1-6(N1)}$, precursor of $\mathbf{P_1}$ can be proposed as the preferred conformation of the biradical 1–6 under UV irradiation. The steady state photoconversion ratio under UV irradiation $[([\mathbf{P_1}] + [\mathbf{P_2}])/([\mathbf{P_0}] + [\mathbf{P_1}] + [\mathbf{P_2}])]_{PSS} = 90 \pm 2\%$ is not sensitive to the 273–313 K temperature change, while the $[\mathbf{P_1}]/[\mathbf{P_2}]$ ratio increases significantly from 0.64 at 273 K to 2.9 at 313 K. It is not easy to interpret this variation on the basis of a unique effect because the six paths are all coupled together. However, it is likely that thermal activation barriers are operating within the photochemical reaction paths [20–22].

Under visible light, both diastereomers are reactive and more significant temperature effects are observed: the rate of process $\mathbf{P_1} \rightarrow \mathbf{P_0}$ increases, while the rate of process $\mathbf{P_2} \rightarrow \mathbf{P_0}$ decreases, when the temperature increases. These trends are the same as observed under UV irradiation. Moreover, in both cases, the rate of photoketonization of $\mathbf{P_2}$ is more temperature sensitive than that of $\mathbf{P_1}$. The lack of $\mathbf{P_1} \leftrightarrow \mathbf{P_2}$ isomerization under visible light is also related to the presence of such thermal barriers. The needed activation energy is easily reached when the biradical intermediates derive from a more energetic excited state (as that reached under UV irradiation) than from a less energetic state formed under visible irradiation. In this last case, $Bi_{1-6(N1)}$ and $Bi_{1-6(N2)}$ do not interconvert each other. As a consequence, it is likely that the thermal activation barriers could be situated at the biradical level.

On the other hand, it is important to note that the behaviour of $\mathbf{P_0}$ is rather different in comparison with derivatives **1** and **2** previously reported [13,14]. No photoenol was detected, suppressing therefore the thermal reversibility underlined with compound **1**. In the same way, no degradation occurred. Two thermally stable diastereomers are formed; there is no evolution to an acridine-dione derivative, as observed with compound **2**. In conclusion, such a compound can be considered as a new photoswitch due to its highly efficient conversion (90%) under UV irradiation and its remarkable reversibility with visible light.

Acknowledgments

The 300 MHz NMR facilities were funded by the Région Nord-Pas de Calais (France), the Ministère de l'Education Nationale, de l'Enseignement Supérieur et de la Recherche (MENESR) and the Fonds Européens de Développement Régional (FEDER). Part of this collaborative work was performed within the framework of the "Groupe de Recherche: Photochromes Organiques, Molécules, Mécanismes, Modèles", GDR CNRS no. 2466.

References

[1] P.G. Sammes, Tetrahedron 32 (1976) 405–422.
[2] P.K. Das, M.V. Encinas, R.D. Small, J.-C. Scaiano, J. Am. Chem. Soc. 101 (1979) 6965–6970.
[3] J.-C. Scaiano, Acc. Chem. Res. 15 (1982) 252–258.
[4] R. Haag, J. Wirz, P.J. Wagner, Helv. Chim. Acta 60 (1977) 2595–2607.
[5] A. Konosonoks, P.J. Wright, M.-L. Tsao, J. Pika, K. Novak, S.M. Mandel, J.A. Krause Bauer, C. Bohne, A.D. Gudmundsdóttir, J. Org. Chem. 70 (2005) 2763–2770.
[6] P.J. Wagner, D. Subrahmanyam, B.-S. Park, J. Am. Chem. Soc. 113 (1991) 709–710;
P.J. Wagner, M. Sobczak, B.-S. Park, J. Am. Chem. Soc. 120 (1998) 2488–2489.
[7] P.J. Wagner, L. Wang, Org. Lett. 8 (2006) 645–647.
[8] A.G. Griesbeck, A. Henz, W. Kramer, P. Wamser, K. Peters, E.-M. Peters, Tet. Lett. 39 (1998) 1549–1552;
A.G. Griesbeck, H. Mauder, S. Sradtmuller, Acc. Chem. Res. 27 (1994) 70–75;
S. Hu, D. Neckers, J. Org. Chem. 62 (1997) 564–567.
[9] A. Zand, B.S. Park, P.J. Wagner, J. Org. Chem. 62 (1997) 2326–2327;
P.J. Wagner, A. Zand, B.S. Park, J. Am. Chem. Soc. 118 (1996) 12856–12857.
[10] J.C. Netto-Ferreira, V. Wintgens, J.-C. Scaiano, Can. J. Chem. 72 (1994) 1565–1569.
[11] D. Lewis, T.A. Hilliard, J. Am. Chem. Soc. 94 (1972) 3852–3858.
[12] K.R. Huffman, M. Loy, M.E.F. Ullman, J. Am. Chem. Soc. 87 (1965) 5417–5423;
W.A. Henderson Jr., E.F. Ullman, J. Am. Chem. Soc. 87 (1965) 5424–5433.

[13] P.H. Gore, J.A. Hoskins, K.A. Lott, D.N. Waters, Photochem. Photobiol. 12 (1970) 551–553;
V.A. Kumar, K. Venkatesan, J. Chem. Soc. Perkin Trans. 2 (1991) 829–834;
T.K. Sarkar, S.K. Ghost, J.N. Moorthy, J.-M. Fang, S.K. Nandy, N. Sathyamurthy, D. Chakraborty, Tet. Lett. 41 (2000) 6909–6913;
J.N. Moorthy, P.R. Mal, R. Natarajan, R.P. Venugopalan, Org. Lett. 3 (2001) 1579–1582.

[14] J. Berthet, V. Lokshin, M. Vales, A. Samat, G. Vermeersch, S. Delbaere, Tet. Lett. 46 (2005) 6319–6324;
J. Berthet, J.-C. Micheau, G. Vermeersch, S. Delbaere, Tet. Lett. 47 (2006) 2485–2488.

[15] V. Lokshin, M. Vales, A. Samat, G. Pepe, A. Metelitsa, V. Khodorkovsky, Chem. Commun. (2003) 2080–2081.

[16] M. Vales, PhD thesis, Aix-Marseille II (2002).

[17] K. Kaps, P. Rentrop, Comp. Chem. Eng. 8 (1984) 393–396;
M. Minoux, in: Dunod (Ed.), Programmation Mathématique, vol. 1, Bordas, Paris, 1983, pp. 95–168;
M.H. Deniel, D. Lavabre, J.C. Micheau, in: J.C. Crano, R.J. Guglielmetti (Eds.), Organic Photochromic and Thermochromic Compounds, vol. 2, Plenum Press, New York, 1999, pp. 167–209.

[18] **P_0**: (^{1}H-NMR, toluene-d_8): 0.87 (3H, t, J = 7.5 Hz, CH_3); 2.16 (2H, q, J = 7.5 Hz, CH_2); 2.57 (3H, s, NCH_3); 4.66 (2H, s, CH_2-2a); 6.69 (1H, d, J = 8.6 Hz, H-8); 6.91 (1H, dd, J = 7.7, 7.5 Hz, H-5′); 6.97 (1H, dd, J = 8.0 Hz, H-6); 7.04 (1H, dd, H-4′); 7.08 (1H, d, H-3′); 7.05 (1H, t, H-4″); 7.15 (1H, dd, H-7); 7.16 (2H, t, J = 7.6 Hz, H-3″ and H-5″); 7.36 (2H, d, J = 7.6 Hz, H-2″ and H-6″); 7.65 (1H, dd, J = 7.5, 1.4 Hz, H-6′); 8.56 (1H, dd, J = 8.0, 1.7 Hz, H-5). (^{13}C-NMR, toluene-d_8): 13.1 (CH_3); 24.2 (CH_2); 32.8 (NCH_3); 39.4 (C-2a); 115.1 (C-8); 123.3 (C-6); 124.2 (C-3); 125.5 (C-4″); 125.6 (C-5′); 127.2 (C-5); 127.4 (C-4a); 128.2 (C-3″ and C-5″); 129.9 (C-2″ and C-6″); 130.3 (C-6′); 130.9 (C-4′); 131.5 (C-7); 131.8 (C-3′); 139.6 (C-1′); 141.4 (C-8′a); 141.8 (C-1″); 142.4 (C-2′); 153.6 (C-2); 175.2 (C-4); 199.0 (C-3a).;
P1: (^{1}H-NMR, toluene-d_8): 0.68 (3H, t, J = 7Hz, CH_3); 1.55 (1H, m, J = 14.3 and 7.2 Hz, CH_2); 1.70 (3H, s, NCH_3); 1.91 (1H, m, J = 14.3 and 7.2 Hz, CH_2); 4.72 (1H, s, H-2a); 6.08 (1H, d, J = 8.6 Hz, H-8); 6.53 (1H, dd, H-6); 6.66 (1H, d, H-3′); 6.94 (1H, dd, H-4′); 6.96 (2H, d, J = 7.6 Hz, H-2″ and H-6″); 7.00 (1H, dd, J = 7.5 and 7.7 Hz, H-5′); 7.01 (1H, dd, J = 8.6 Hz, H-7); 7.13 (2H, dd, J = 7.6Hz, H-3″ and H-5″); 7.16 (1H, t, H-4″); 8.10 (1H, dd, J = 7.8 and 1.8 Hz, H-5); 8.19 (1H, dd, J = 7.6, 1.7 Hz, H-6′); 17.85 (1H, s, OH). (^{13}C-NMR, toluene-d_8): 8.9 (CH_3); 27.7 (CH_2); 34.5 (NCH_3); 61.1 (C-2a); 68.0 (C-2); 106.8 (C-3); 111.4 (C-8); 115.4 (C-4a) 116.3 (C-6); 125.1 (C-5); 126.4 (C-6′); 127.0 (C-5′); 127.7 (C-3″ and C-5″); 128.0 (C-3′); 129.6 (C-4″); 130.2 (C-1′); 132.4 (C-4′); 133.9 (C-2″ and C-6″); 134.9 (C-7); 140.7 (C-2′); 141.9 (C-1″); 151.3 (C-8a); 174.8 (C-4); 182.1 (C-3a).;
P2: (^{1}H-NMR, toluene-d_8): 0.77 (3H, t, J = 7.3 Hz, CH_3); 1.61 (2H, q, J = 7.3 Hz, CH_2); 2.31 (3H, s, NCH_3); 3.99 (1H, s, H-2a); 5.94 (1H, d, J = 8.4 Hz, H-8); 6.40 (1H, dd, J = 7.8, 7.0 Hz, H-6); 6.76 (1H, t, J = 7.2 Hz, H-4″); 6.82 (2H, dd, J = 7.2, 7.1 Hz, H-3″ and H-5″); 6.88 (2H, dd, J = 7.0, 8.4 Hz, H-7 and d, H-3′); 6.94 (1H, dd, H-5′); 6.97 (1H, dd, H-4′); 7.29 (2H, d, J = 7.1 Hz, H-2″ and H-6″); 8.00 (1H, dd, J = 7.8, 1.8 Hz, H-5); 8.18 (1H, dd, J = 7.6, 1.8 Hz, H-6′); 18.1 (1H, s, OH). (^{13}C-NMR, toluene-d_8): 8.9 (CH_3); 30.6 (NCH_3); 35.8 (CH_2); 56.4 (C-2a); 66.3 (C-2); 102.6 (C-3); 109.9 (C-8); 115.2 (C-4a); 116.2 (C-6); 126.4 (C-5); 126.7 (C-4″); 126.8 (C-6′); 127.4 (C-5′); 128.3 (C-3″ and C-5″); 128.4 (C-2″ and C-6″); 129.1 (C-3′); 130.1 (C-1′); 132.9 (C-4′); 135.2 (C-7); 141.3 (C-1″); 142.0 (C-2′); 150.4 (C-8a); 176.0 (C-4); 182.1.(C-3a).

[19] 1,4-Biradical if produced would rearrange very rapidly into 1,6-biradical.

[20] E. Fischer, J. Am. Chem. Soc. 82 (1960) 3249–3252.

[21] S. Malkin, E. Fischer, J. Phys. Chem. 66 (1962) 2482–2486.

[22] S. Malkin, E. Fischer, J. Phys. Chem. 68 (1964) 1153–1163.